Environ Monit Assess (2021) 193:640
https://doi.org/10.1007/s10661-021-09433-z

Reservoir bathymetry and riparian corridor assessment in two dammed sections of the Teesta River in Eastern Himalaya

Alex. J. Fields · Joydeep Bhattacharjee · Nirmalya Chatterjee

Received: 29 March 2021 / Accepted: 30 August 2021

Abstract As of mid-2021, four hydroelectric dams are operational on the main channel of the Teesta River in the mountainous and tectonically active Sikkim-Darjeeling-Kalimpong region of India. Riparian ecological and fluvial morphological changes after damming have not been documented. This paper describes an early study of a section of the middle Teesta River, at two of the dam-created reservoirs, just before the river enters the plains. High-resolution, multi-beam, geo-located sonar was used to map the bathymetry of the reservoirs. This resulted in the creation of 30cm-resolution bathymetric maps of the two reservoirs showing valley bottom morphology within them. The bathymetric maps were compared with pre-dam digital elevation models of the valley to create topographic change-maps. The change-maps indicate significant differences in valley morphology due to erosion and deposition processes. Land cover changes due to inundation were quantified from analysis of satellite imagery time series data of the reservoir riparian zones. Land cover change analysis showed a loss of ~ 74,000 trees in ~ 225 ha of flooded riparian corridors due to long-term inundation. The study shows that the dams have caused 7.4% of the river length to become quasi-lentic, and drastically altered sediment dynamics and hydrologic flow. Sediment deposition calculations indicate the reservoirs losing almost three-quarters of their surface areas to sediment deposition features within 15 years. This study will serve as an important baseline for future studies, and influence design and policy regarding riparian and fluvial ecosystem management, monitoring, and evaluation in the Teesta and similar mountainous river basins in the Eastern Himalaya.

Keywords Fluvial geomorphology · GIS · Forest inundation · Sediment build-up · Erosion–deposition

A. J. Fields
Department of Forestry and Natural Resources, Purdue University, 195 Marsteller Street, West Lafayette, IN 47907, USA

J. Bhattacharjee (✉)
Plant Ecology Lab, Biology Program, University of Louisiana - Monroe, 700 University Avenue, Monroe, LA 71209, USA
e-mail: joydeep@ulm.edu

N. Chatterjee
Eastern Himalaya-NE India Regional Office, Ashoka Trust for Research in Ecology and the Environment (ATREE), Tadong, NH-10, Gangtok 737102, Sikkim, India

Introduction

Glacial snow-fed rivers begin their course downstream from the upper reaches and create steep valleys by the erosive power of fast-moving water and the rocky debris carried along with it (Franzle, 1997; Seret, 1997). Large rocky debris, small boulders, and coarse gravel are deposited along the steep river channel at its upper reaches. The suspended or transported

Published online: 10 September 2021

sediments (sub-micron clay and gravel a few tens of millimeters across) are carried by the water further and are deposited partially along the river beds and banks where stream velocities are lower, commonly in the riparian zones and flood plains, and along the downstream plains (Aslan, 2003; Bruun, 1997). This process is integral to soil-building activities in the alluvial plains and the delta (inland or estuarine) of a river (Coleman, 1997; Schmudde, 1997). Dam building drastically changes the hydrologic regime of the river and the reservoir segments of the river change from a lotic to a quasi-lentic system (Marsh & Fairbridge, 1999).

A fast-moving river tends to lose its easily transported sediments upstream of the dam due to abrupt velocity and kinetic energy dissipation. This leads to depositional feature formation in the upper reaches of the created reservoir due to the drop in sediment carrying capacity (Nanson & Gibling, 2003). Only very fine, suspended sediments (fine silts and clays) make their way further downstream into the reservoir and beyond. Much of the finer sediments also end up depositing within the reservoir area; either at the valley bottom or along the shorelines. These finer sediments then rapidly fill the reservoir, and unless removed and mobilized in some manner, deprive the lower course of the river and delta of new sediment while reducing reservoir storage capacity (Jain et al., 2009). In the case of Himalayan rivers, the upper course features the highest amount of weathering activity (Harris et al., 1998) and the effects of damming may result in both lowered weathering and sediment creation as well as a concentration of weathered materials in the impounded, confined valley itself.

Recent research in India on dammed rivers has been based on remote sensing imagery. While remote sensing-based studies offer easy coverage of relatively inaccessible terrain, however, drawbacks including technical issues like topographic shadowing in hilly regions and lack of useable data due to cloud cover that blocks the spectral line of sight of satellite-based sensors during monsoons. In the case of the Himalayan region, both these factors are of particular concern.

A study of the Godavari River delta in southern India found large scale erosion causing the evacuation of coastal communities, due to the ingress of the sea and loss of mangrove forests (Malini & Rao, 2004). Studies on the Krishna River delta reported coastal erosion due to the reduction in water flows and sediment flux (Panda et al., 2011). Similarly, the upstream damming of the Narmada River has resulted in a significant reduction in sediment flux into the Arabian Sea (Gupta & Chakrapani, 2005). Sediment deposition studies at the Three Gorges Reservoir in China have also indicated a complex relationship of erosion and deposition using subsidiary dams on tributaries and higher-order stream check-dams (Gao et al., 2015). Long periods of coastal erosion were predicted in California due to the more than 500 dams reducing annual soil and gravel flux in the region by up to 25% (Willis & Griggs, 2014). A study of the Tiga Dam in Nigeria on the Kano River ten years after construction found channel reduction, with widths falling from 249 to 34 m, and depth from 2.01 to 1.44 m (Olofin, 1988).

The southern Sikkim-Darjeeling landscape forms part of the Lesser Himalaya foothills with a complex topography and is under heavy cloud cover for up to half the year. A thorough study thus requires ground-level monitoring and evaluation of the terrain with supporting data from available remotely sensed datasets.

This study is an early attempt to assess the status of about a 21-km impounded section of the Teesta River's middle course, just before the river debouches into the plains at Sevoke Town in West Bengal, India. The study resulted in creating baseline bathymetric maps of the reservoirs (formed due to the TLD3 & TLD4 dams, Figs. 1 and 2), quantifying potential sediment build-up in the reservoirs, and collecting data on land and forest cover loss to document the changes to the river's fluvial, geomorphological, hydrological and riparian ecological characteristics following damming.

Materials and methods

Study site

The Teesta River is fed by meltwaters from the Zemu (NW Sikkim), the Teesta Khangse (NE Sikkim) glaciers, the snow-fields of the Khangchendzonga and Pauhunri massifs, and the trans-Himalayan high-altitude lakes of Gurudongmar and Tso Lhamu (all in the North Sikkim district). The main tributaries of

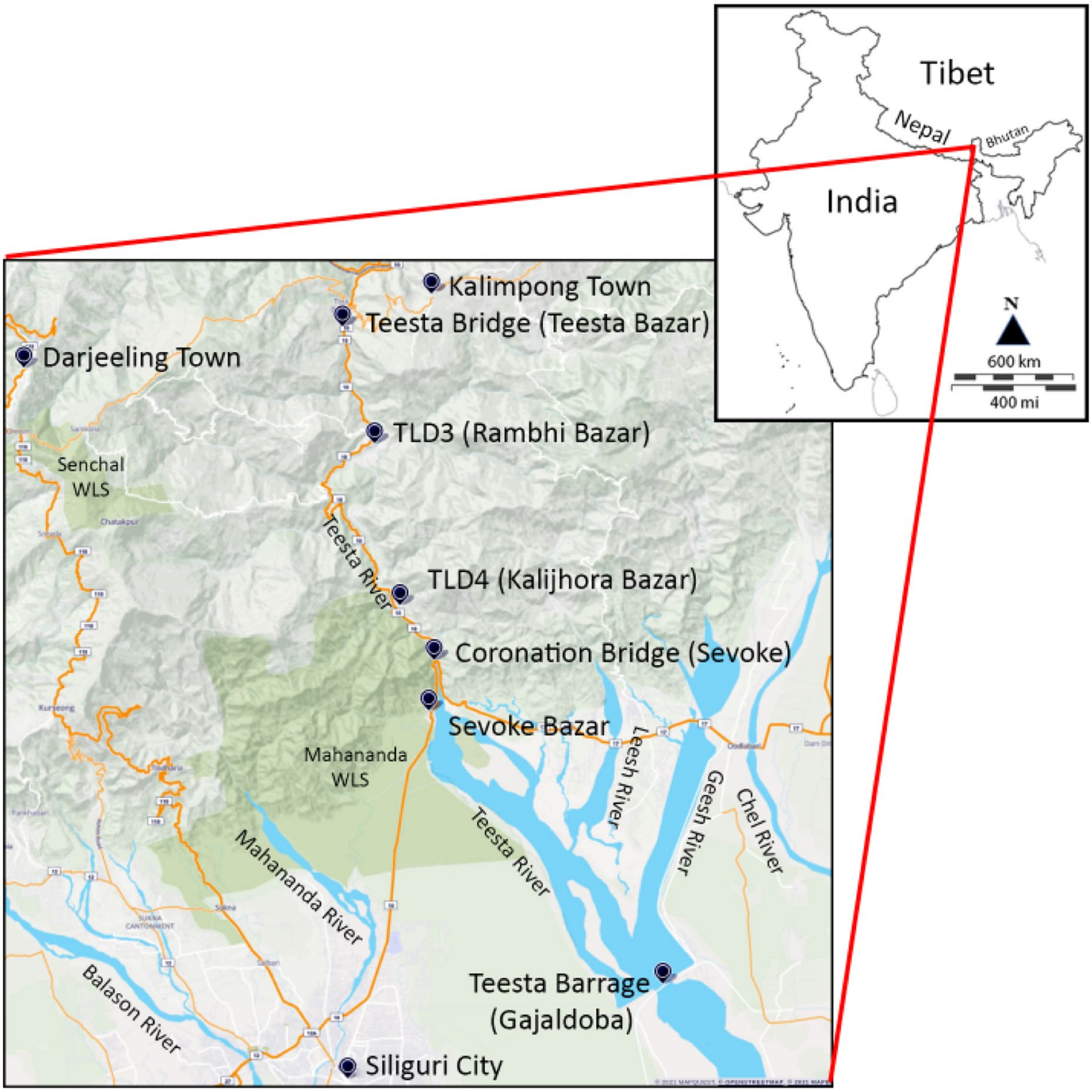

Fig. 1 Map showing the location of study sites on the Teesta River including the nearby habitations, landmarks, and rivers, in the mountainous Darjeeling-Kalimpong region of West Bengal, India. Inset shows location of the study site within India

the Teesta are the Rangeet River (draining northern Darjeeling and West Sikkim districts), the Lachen Chu (draining western North Sikkim district), and the Rongpo Chu (draining East Sikkim and northern Kalimpong districts). Numerous smaller tributaries also contribute to draining a basin area of 12,540 km^2. The basin includes most of the state of Sikkim, northern portions of the Darjeeling and Kalimpong districts, and western parts of Jalpaiguri district in the state of West Bengal in India, before the Teesta flows into the Brahmaputra River, near Chilmari in Kurigram district (Rangpur division) of Bangladesh. The upper Teesta basin is part of the Eastern Himalaya which is one of 34 global biodiversity hotspots (Myers et al., 2000). The Teesta river provides habitat for 92 fish species (Acharjee & Barat, 2013; Bhatt et al., 2017) including the critically endangered *Tor putitora* (Golden Mahseer) (Allen et al., 2010). While

Fig. 2 Schematic showing landmarks, human settlements, headwaters, catchment areas, and tributaries of the upper Teesta River basin in the Sikkim-Darjeeling-Kalimpong region with respect to the study sites

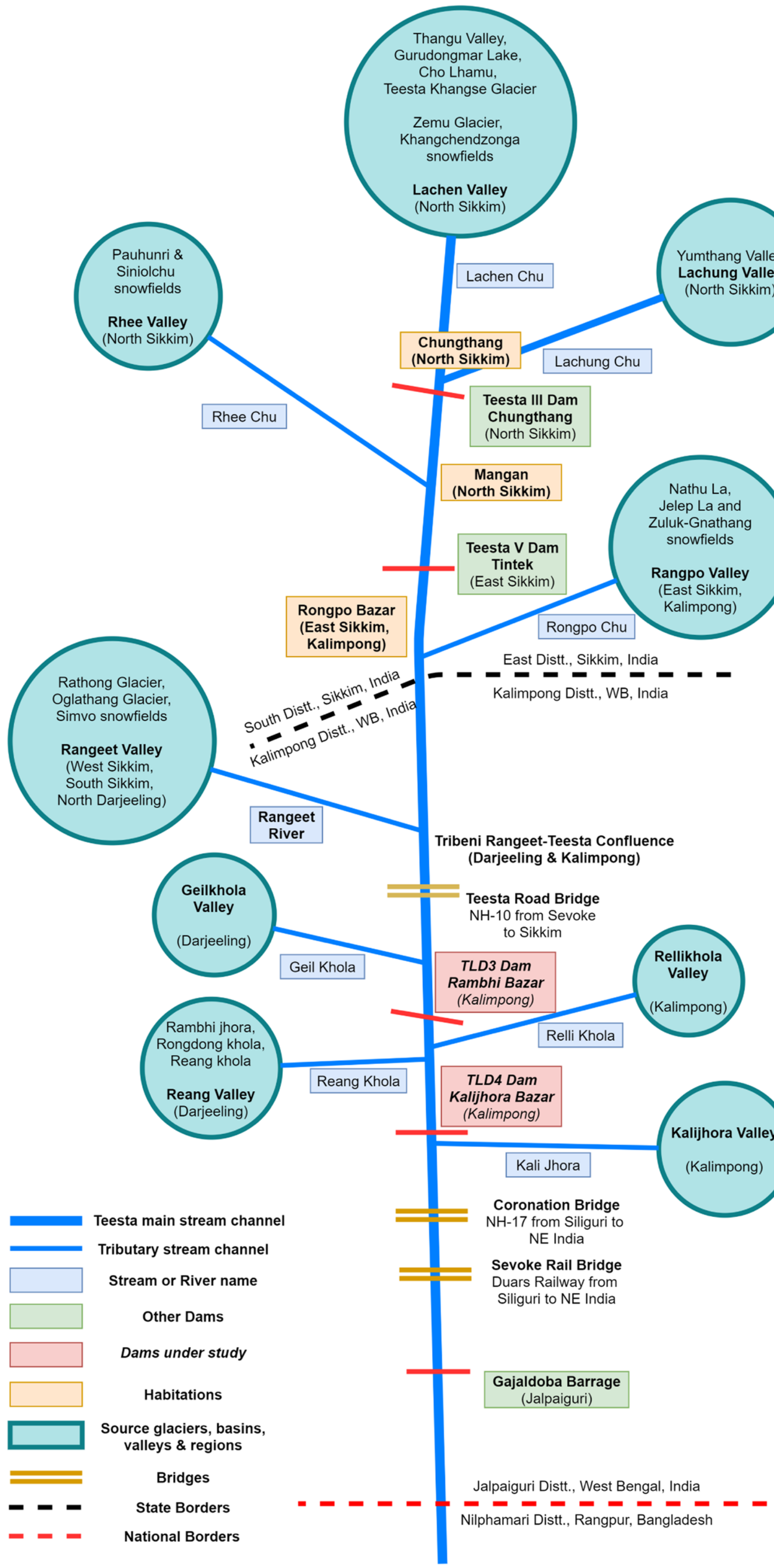

biodiversity assessments have been undertaken in the lower course of the Teesta River; assessments of changes in valley morphology and local terrain, which need large-scale, high-resolution survey data, are absent (Adhikari et al., 2019; Islam & Sarker, 2017).

The details of the currently operational dams on the main stream of the Teesta River are given in Table 1. The two dams studied (Teesta Low Dam III and IV—hereafter TLD3 and TLD4) are in the state of West Bengal, India (Fig. 2) and are officially classified as 'low' dams (height below 50m) even though there is a substantial alteration in hydrological flow due to them. The two dams considered in this study resulted in the creation of 21.2km serpentine reservoirs on the Teesta River which has resulted in the inundation of riparian corridors on both banks. The dams are about 12 km apart by the river. There are several smaller dams planned or completed on the tributary streams (Mehta, 2013). There are no records of mitigation activities except hillside reinforcements through concrete injections and embankments near the dams, undertaken to alleviate the potential impacts these dams may have on the riparian ecosystem of the Teesta River (pers comm NHPC management, 2018). Large-scale topographical changes are also occurring due to repeated landslides in the riparian zone and near catchments along the reservoir banks during the rainy season (SANDRP 2020; The Telegraph (Kolkata), 2020; The Deccan Herald (Bengaluru), 2015).

The TLD3 and TLD4 dams are the focus of this study because these were recently commissioned (in 2013 and 2016, respectively), relatively easily accessed from the nearby highway, and are not under areas with restrictive border management (e.g., dams in Sikkim). With just a few years passed after the commissioning of the second dam, they are both still considered early in a dam's design lifetime, and the initial impacts of these dams on the ecosystem are beginning to show. The two dam reservoirs are separated enough to serve as spatial replicates, especially in evaluating the changes due to the impounding of the river, inundation of the former riparian areas, and episodic water movement in the shorelines of the current reservoirs. The basic flowchart of the methods and outputs used is shown in Fig. 3.

Until recently, in the Himalayan reaches, the Teesta River was a fast-flowing stage 1 river with no flow impediments and was ecologically a lotic system year-round, until it reached the plains of West Bengal where lock gates divert water for irrigation. Now, with the construction of dams along its course, long stretches of the river have standing water all year-round and ecologically resemble quasi-lentic systems, with flows below the dams considerably reduced. The formation of reservoirs has caused the inundation of the valleys upstream of each dam. As a result, the banks currently extend well past the original floodplain into forested areas beyond the historical banks and associated riparian zone.

Table 1 Details of the operational hydroelectric dams on the main channel of the Teesta River (as of 08/2020)

Project official name operator	Commission date (mm/yyyy)	Location [Location, District, State] (Lat, Long)	Dam height & generation capacity
Teesta III Teesta Urja[a]	02/2017	Chungthang, North, Sikkim (+27.597874°, +88.650076°)	60 m 6×200 MW
Teesta V NHPC Ltd[b]	03/2008	Tintek, East, Sikkim (+27.386974°, +88.503643°)	88. 6 m 3×170 MW
Teesta Low Dam III (hereafter TLD3)[c] NHPC Ltd	02/2013	Rambhi Bazar, Kalimpong, West Bengal (+27.002045°, +88.442549°)	32 m 4×33 MW
Teesta Low Dam IV (hereafter TLD4)[c] NHPC Ltd	05/2016	Kalijhora Bazar, Darjeeling, West Bengal (+26.928013°, +88.456126°)	45 m 4×40 MW

[a]60% owned by the Govt. of Sikkim

[b]National Hydroelectric Power Corp. Limited, 71% owned by Govt. of India

[c]Reservoirs surveyed in this study

Fig. 3 Flowchart of basic methods employed for generating outputs of inundation, bathymetry, and lifetime maps of the Teesta Low Dam reservoirs used in this study

Bank inundation and land cover analysis

The land cover change was analyzed using image classification as a time series analysis technique in ENVI (version 5.5): an image analysis software used to extract information from imagery. LandSat satellite imagery of the two dam sites in their pre-dam (2011) and post-dam (2018) states was acquired. The images were clipped using regions of interest (ROI) polygons. Land cover was classified as either land (grey), or as water (blue) through supervised classification using pixel selection on the raster imagery. The image classification workflow was used to train ENVI to recognize pixels in the satellite imagery as land or water and pixels within each class were quantified. Land lost to inundation was calculated by subtracting pixels in classified images between 2011 and 2018 for both reservoirs. The product of pixel count with the pixel size of 900m^2 and results are reported on a per hectare (ha) basis. An on-ground count of trees was carried out by sampling trees in 10 × 10m plots that were randomly placed along the riparian zone of the river. All trees were manually counted within each plot and the process was repeated at fifty-four (54) different plots on both banks of the reservoirs.

Bathymetry

Sonar imagery from within the reservoir areas (Fig. 4) show an example visual of the cross-section of the river. It depicts the original floodplain filled in with sediments and fully grown trees submerged, several meters from the historic riverbank. Currently, upstream of the dams, the river alternates between periods of no or reduced flow, depending on whether the dam sluices are open or closed.

Sonar bathymetry was conducted using multiple transects on an 8805-m stretch upstream of the TLD3 and an 8490-m stretch upstream of the TLD4 between May 2018 and June 2019. The upper boundary of the TLD3 reservoir reaches the Teesta-Rangeet river confluence, depending on the season and dam closure timings, while the upper limit of the TLD4 reservoir is about 1200-meters downstream of the TLD3 dam, just south of the Teesta-*Reang Khola (river)* confluence. Each reservoir site was divided into three reaches (lower, middle, and upper) starting around 1 km upstream of the corresponding dam. A closer approach was not permitted by the dam operators due to safety and security protocols. A reach was defined as a third of the total surveyed length of the respective reservoir.

Bathymetry and water sampling data were collected from an electric motor-powered raft (Intex Mariner 4 with a Minn Kota Endura C2, Max thurst 30-lb trolling motor) equipped with a Garmin echoMAP 73SV chart plotter and a chirp-signal capable, multi-beam sonar transducer unit (Garmin CV52HW-TM) mounted 30 cm away from the propellers, under the raft. This set-up allowed real-time collection of geo-located, water depth, and water temperature data. The chart plotter also shows real-time sonar-based cross-sectional imagery of the reservoir bottom. Garmin Quickdraw Contour software installed in the chart plotter also created bathymetric maps at 30 cm contour intervals and was used to

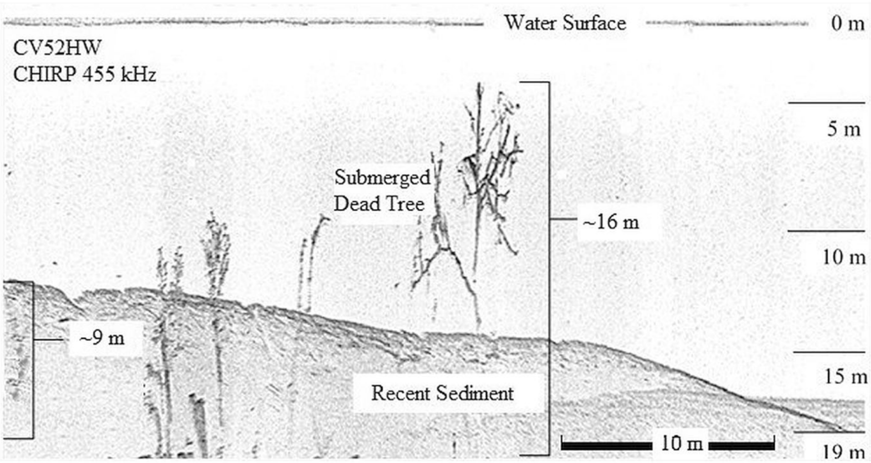

Fig. 4 A cross-sectional sonar view of the river sediment and water column showing new sediment deposits and submerged dead trees

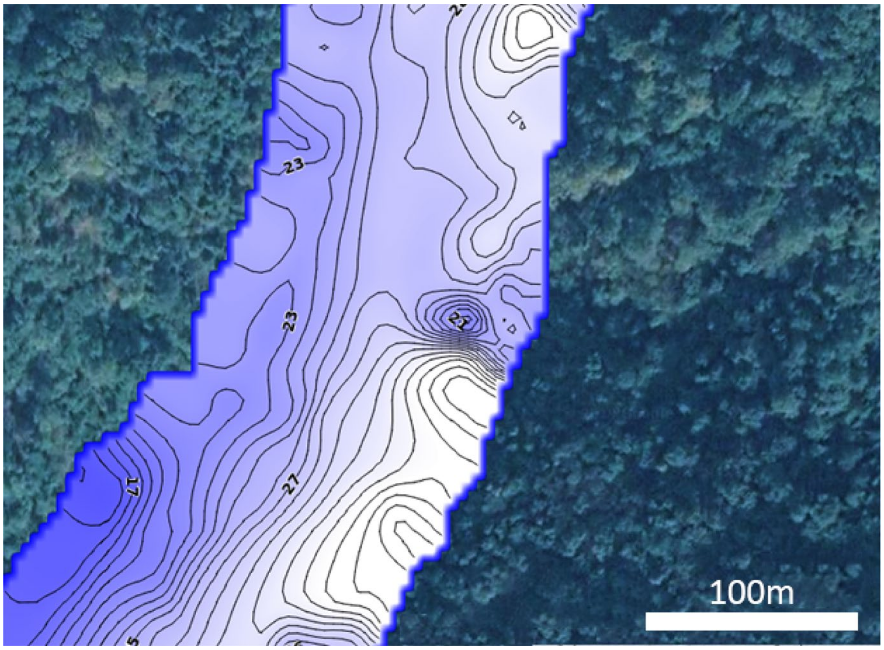

Fig. 5 Bathymetric contours of a section of the reservoir superimposed over visual satellite imagery

create real-time, high-resolution depth and coverage maps, thus ensuring complete coverage of the reservoir surface (Fig. 5). The water levels were base-lined with height markers in the upstream shore prior to the survey trips. For the TLD3 reservoir, the water level markers maintained by the NHPC on the west pylon of the Teesta River Road bridge was used to calibrate the day's water level before the survey. For all other water levels, local on-shore landmarks were used at fixed GPS coordinates.

The width of the channel and prevailing water turbidity dictated the number of transects required for complete coverage. In most places, three parallel transects (two close to either bank and one at the channel center) were sufficient for complete coverage. Additional smaller transects were run at the wider sections of the river for a complete bank to bank coverage. The chart plotter-transducer recorded geographic coordinates, water temperature, and depth values of the reservoir at 15-second intervals using its in-built software.

Final bathymetric maps of the study sites were created by combining data from transects to create a geo-located, point-cloud layer of water depths in ArcMap 10.7. The Geostatistical Analyst extension was used to interpolate water depths and create a continuous, equally spaced raster layer of water depth for the two reservoirs. Different kriging and interpolation methods were tested for error residuals, and coverage, interpolation and contour artifacts, and continuity. The testing showed that *Ordinary Kriging* gave the lowest interpolation residuals and best performance at near shore-edges and across abrupt depth change areas. The krigged, bathymetry raster layers were subsequently clipped to high-water mark contour lines of the respective reservoirs.

Valley-bottom sediment accumulation

The bathymetry raster data layers created using kriging were further used to make high-resolution terrain model rasters of the valley bottom after inundation due to the dams. The base map (pre-inundation) rasters were created from the MERIT DEM dataset (Yamazaki et al., 2017).

The MERIT product is based on SRTM3, which itself is based on SRTM2 that uses only the non-void-filled version of the original SRTM data. The void areas of SRTM2 were filled with a combination of the following elevation data: stereo photogrammetry-based data from NASA Terra satellite (ASTER GDEM), 12.5m-resolution JAXA ALOS 3D data (stereo photogrammetric), and 60m-resolution NASA ICESat Laser Altimetric (LiDAR), to avoid the use of interpolation. The MERIT dataset also uses multi-channel and multi-aspect flow algorithms for assigning hydrologically coherent flow direction and accumulation. The basic premise of the MERIT product was to create a DEM product with the least possible use of interpolation with hydrological consistency. We chose it over others to meet the needs of our research focus.

A post-inundation water surface layer was added in the MERIT DEM based on the respective reservoir's high watermark (220m for TLD3, 202m for TLD4). The bathymetry depths were then deducted from this water surface polygon to create a post-inundation valley bottom DEM. This gave us a reasonable approximation of the changes in the valley bottom due to erosion-deposition processes. Assuming similar trends in catchment level sediment export, it gave us a method to calculate the tentative time taken for visible sediment deposit bars to show up mid-stream, on a cell-sized (pixel) water column in the reservoirs. Such sediment bar formation is already visible during low water levels in the reservoirs during the annual monsoonal high-flow season (June-September) when the dam gates are fully opened and by the presence of mid-stream shallows observed during our bathymetry data collection runs in the post-monsoon season (November–January).

Results

Bank inundation

Much of the riparian regions above the old floodplain have been impacted due to the building of concrete embankments, bank-and-hillside reinforcement using concrete injections, hillside and bank weakening due to lateral water ingress or surficial inundation, or combinations thereof. Significant swathes of riparian forest trees are now to be found dead and decaying within the reservoir (Fig. 6).

Analyses of image classification used to quantify the changes in water surface cover of both dam sites from pre-damming (2011) to post-damming (2018) showed that land cover changes due to the TLD4 reservoir were greater than that due to the TLD3 reservoir, due to significant widening of the river valley immediately downstream of TLD3 and the confluence of the rivers *Reang Khola* (west) and the *Relli Khola* (east). Inundation due to the TLD3 reservoir is about half that of the inundation due to TLD4.

The reservoir-wise analysis and classification of the land cover into two categories, namely, land and water are shown in Table 2. A pixel count of the two categories indicated conversion of ~75ha (TLD3) and

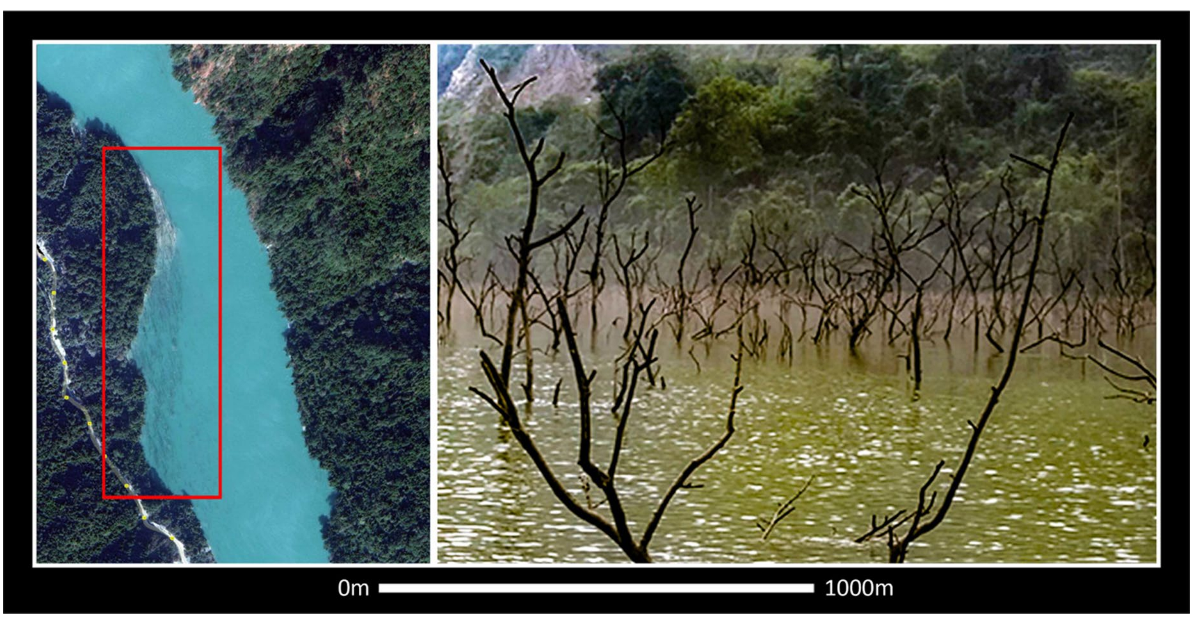

Fig. 6 An example of forest tree loss in the study area. Aerial (left) and on-site (right) views of a dead forest in an inundated, former riparian zone within the TLD4 reservoir (+26.955818°, +88.438514°). Note: Scale refers to aerial image, on the left

Table 2 Results of image classification of the Teesta Low Dam study sites in West Bengal, India

Site	Cover class	Year	Total class-wise Pixel count (px)	Training pixels	Δ Area (ha)
TLD3	Land	2011	18,504	1142 (2011)	−75.42
		2018	17,666	1111 (2018)	
	Water	2011	756		+75.42
		2018	1594		
TLD4	Land	2011	21,636	1538 (2011)	−149.67
		2018	19,973	1509 (2018)	
	Water	2011	1037		+149.67
		2018	2700		

Raster resolution was 30 m, resulting in a pixel area of 900 m^2

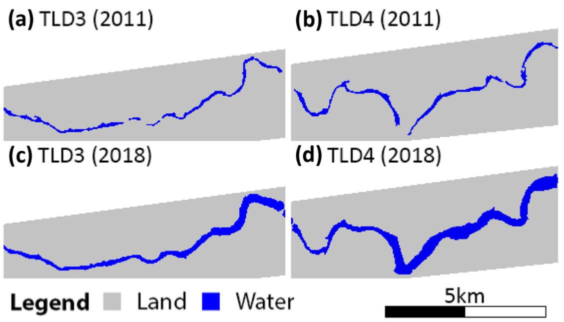

Fig. 7 Inundation and associated land loss in riparian zones along with the newly formed reservoirs due to damming, based off of land cover classification from 30 m resolution LandSat imagery using ENVI 5.5

~150ha (TLD4) of land into water category due to dam-induced submergence along the two reservoirs. Together both dam sites have lost 225 ha of riverbank forest, gravel beds, and floodplains post-damming. The inundation of the former floodplain and upland areas at the dam sites between 2011 and 2018 are visible at both sites (Fig. 7).

Canopy-level tree loss count

The average tree count along the riparian corridor was 3.28/100m^2 plot (328/ha, ± 24.7 SE) in the 54 study plots, obtained from the field vegetation survey. As per standard vegetation sampling protocol, a tree was included in the count only if it measured greater than 10cm diameter at breast height (DBH). A total of 73,830 trees were lost due to submergence and prolonged inundation of the bank and upland forest by the two reservoirs.

However, the limits of using this approach did not account for the estimation of any other vegetation categories including juvenile trees, woody lianas, shrubs, and herbaceous plants that were lost due to dam-induced inundation of the Teesta River's banks. Further, it should be noted that these riparian areas also provided habitat for a diverse faunal species. It also does not account for the presence of potentially large, in-forest stretches of gravel and sediment beds, something that is common in such riparian areas, even without the presence of dam-induced flooding.

Bathymetry

Overall, water depth increased as the river approached the dams. The bathymetric maps of both TLD3 and TLD4 showed an increasing water depth gradient downstream (Fig. 8). The minimum depth at TLD3 and TLD4 were close to the riverbank (0.2 and 0.3m, respectively), and the maximum depths of the reservoirs were at their lower reaches (23.8 and 28.6m, respectively).

Comparisons between the study sites pre-dam and post-dam show overall lower depths (higher elevation values) in 2019 than that in 2011, indicating significant sediment build-up of the inundated, valley bottom. Even a cursory view (Fig. 9) shows the resulting flat-bottoming not typical of such fast-flowing, mountain rivers, which typically have a V-shaped valley.

Estimates of the average depth at each reach of the two study sites are displayed in Fig. 9. Pre-damming, the maximum predicted water depth at the TLD3 site was 9.4m as opposed to 23.8m post-damming; and the maximum at the TLD4 site was 13.7m as opposed to 28.6m.

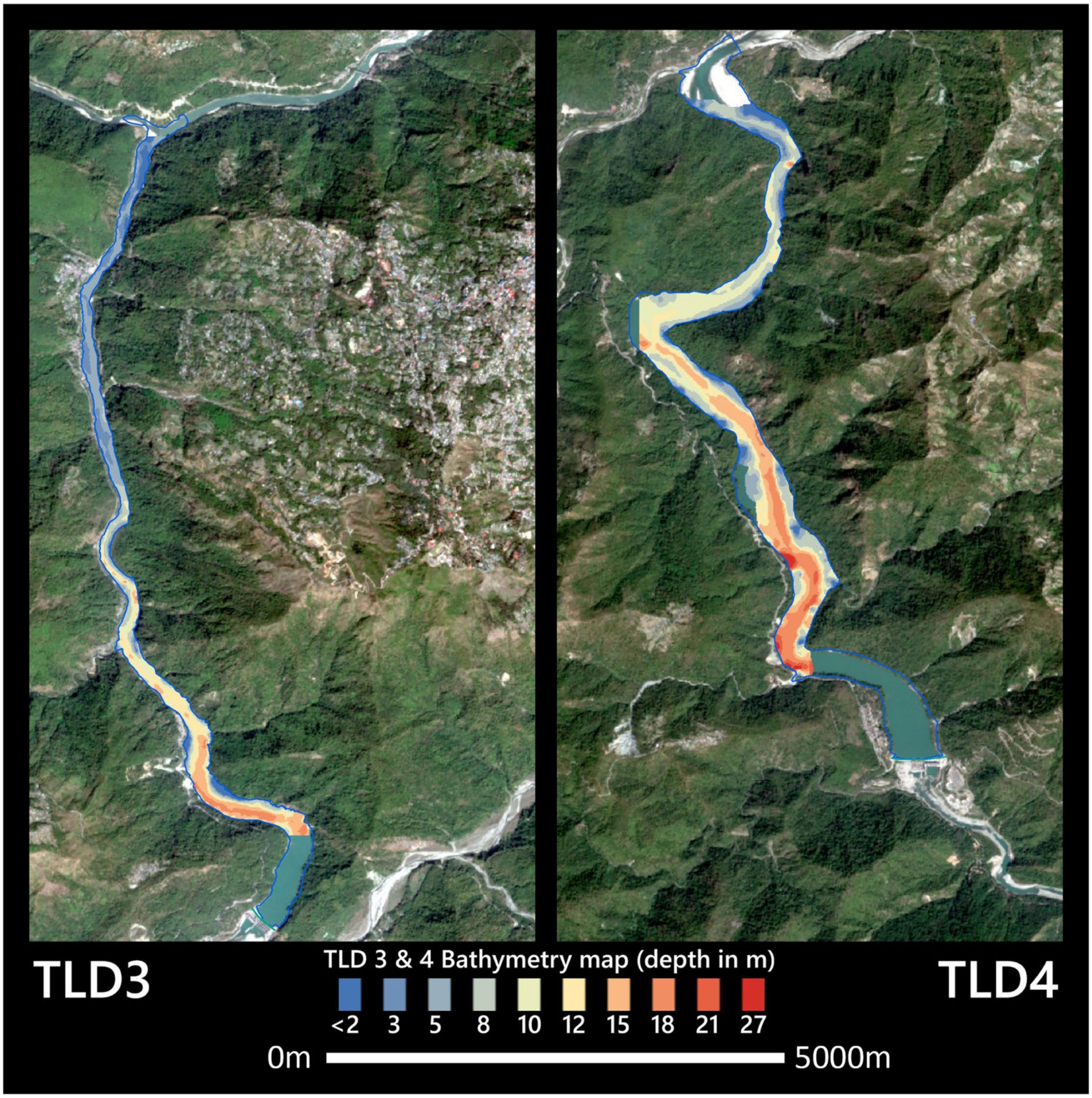

Fig. 8 Interpolated bathymetry maps of surveyed areas of the study sites (left) Rambhi Bazar, TLD3, (right) Kalijhora, TLD4, superimposed over visual satellite imagery

Comparisons of the tentative timelines for coverage of the reservoir surface with visible depositional features are reported in Table 3. It provides an easily understood process-based assessment of the reservoir capacity and its contribution to the power generation and flood regulation capacity of the dams.

Valley-bottom sediment accumulation

The pair of valley bottom terrain models for pre-inundation and post-inundation for the two reservoirs are shown in Fig. 9. The calculations of sediment build-up within the reservoir areas are based on valley bottom terrain models available

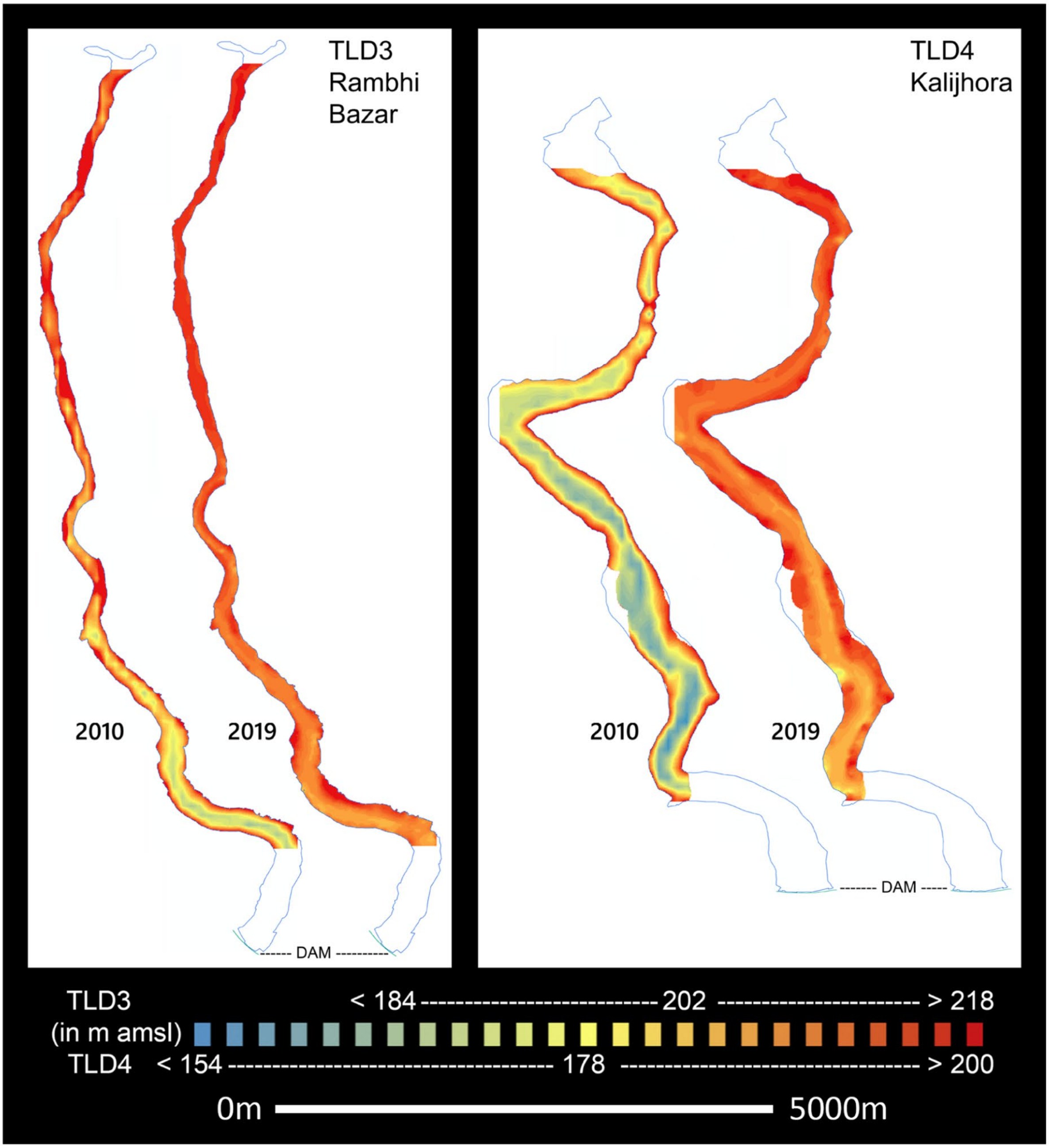

Fig. 9 Valley-bottom morphology changes before and after commissioning of the Teesta Low Dam—TLD3 and TLD4, showing noticeable valley bottom flattening due to ongoing erosion–deposition processes after valley inundation. Elevation values of the valley bottom are in meters above sea level

from pre-inundation (2011) digital elevation data and post-inundation (2018–19) bathymetry data. This allows for calculating the rate of sediment deposition and an estimated time for these deposits to become visible on the surface as sediment bars.

Table 3 Comparisions of pre-dam DEM and bathymetry raster calculations on the Teesta Low Dam reservoirs

	Percentage area coverage by feature-class over reservoir lifetime (years)	
Years	TLD3	TLD4
Depositional features		
0–5	10.925	59.451
5–10	28.965	26.175
10–15	30.714	2.303
15–20	6.400	1.006
20–25	2.747	0.501
25–30	1.444	0.287
30–35	0.942	0.268
> 35	3.979	0.994
Erosional features[a]		
	3.884	9.016

Years to fill-up the available reservoir capacity calculated based on known reservoir ages (73 months for TLD3 and 37 months for TLD4) as of June 15, 2019

[a]Coverage of erosional features calculated by subtracting the total coverage of depositional feature classes from 100

In the upstream TLD3 reservoir, up to *71% of the reservoir area* may show visible sediment bar formation during low water levels within the next 15 years (2031), for the downstream and generally shallower TLD4 reservoir up to *88% of the reservoir area* may show visible sediment bars in the next 15 years (2027).

However, there exists a multitude of depositional processes within the reservoirs. Processes like aggravated medium and fines deposition due to reduced sediment carrying capacity of the main Teesta River, contribution to fine sediments from direct tributary streams, coarse and rocky debris flows into the reservoirs due to large scale mass movements in the surrounding and submerged hillslopes, and extreme precipitation-driven landslide, rockslides, and mudflows—all of which contribute to deposition in the reservoir. It is impossible to apportion or predict the contributions of each of these processes in multi-decadal timelines without further studies primarily emphasizing these processes.

Discussion

Bank inundation

Using image classification and pixel counts, it was found that about 225 ha of the riparian corridor has been lost since the commissioning of TLD3 and TLD4. Additionally, TLD4 has led to a loss of nearly double the amount of land as TLD3 has since 2011. The reservoirs are the widest just upstream of the dam at both study sites (Fig. 8). The effects of inundation can be predicted to be lowest far upstream of each dam where parts of the riparian corridor and banks are still intact, and highest downstream, close to each dam where the original banks are all but absent, and the loss of riparian area is the most severe. Also, this may be an evidence that in rivers where consecutive dams are constructed, land loss will be higher at the dam that is further downstream.

The large difference in land loss between the two dam sites might also be influenced by the difference in heights between the two dams. The taller height of TLD4 creates a larger reservoir. The reservoir of TLD4 has inundated large patches of upland terrain in addition to the riparian corridor and has left behind thousands of dead standing trees along its lower reach (Fig. 6). These would have been mature trees at heights of over 15m tall. This phenomenon is unique to TLD4 where a floodplain is now absent and the water from the reservoir rises even up the cliff faces of the valley. This is concerning because the upland cliffs are composed of layers of friable phyllosilicate rocks, and water ingress-driven exfoliation at depths makes the cliffs vulnerable to landslides. A review of historic landslides found a strong correlation with reservoir formation (Petley, 2013). While most events are common immediately after dam construction, however later on water-ingress-driven weakening and subsequent hillslope failure are also documented decades after construction. This supports the finding that the Teesta valley is at risk of landslides years after dam construction (Pradhan et al., 2015). According to public testimony in the Teesta valley, increased landslides are responsible for interrupting traffic on NH-10, the only major highway that connects the state of Sikkim to the rest of India.

Increased incidences of catastrophic flooding after heavy monsoon downpours are also common in the Eastern Himalaya. The plains town of Jalpaiguri was flooded when the Gajoldoba Barrage was breached by a monsoon cloudburst in 2015 (Pal et al., 2016). Climate change poses a risk of increasingly frequent flash floods in the region since the Teesta is primarily glacial melt and monsoon fed. Changes to precipitation patterns may drastically change the catchment scale water budgets (Goswami et al., 2006). A study of 51 households in the towns of *Geil Khola* Bazar and Baluwakhani, both along the TLD3 reservoir, found that 90% of residents feel unsafe living near the reservoir (Wiejaczka et al., 2018).

Bathymetry

Bathymetric maps of both dam sites still show near-identical trends in water depths from the upper reaches to the lower reaches, with the deepest portions immediately upstream of the dams. However, the amount of sediment build-up is noticeably more within the TLD4 reservoir (Fig. 9). Typically, as a river cuts its path through the landscape, weathering is greatest at the banks and the valley bottom at the center of the channel, creating a V-shaped cross-section (Kiss et al., 2008). Extensive inundation combined with the formation of multiple reservoirs along its length is reshaping the valley. The original banks no longer contain the river's channel as the water now permanently flows over what used to be its floodplains and riparian corridor (Fig. 6). The sediment deposition at the bottom of the reservoirs is changing the valley bottom morphology, with minor topographical aberrations getting filled out with deposits, and the valley taking up a flat-bottomed shape.

With a total of 18 dams planned to be constructed on the river, therefore the effects of dams on the Teesta River need to be understood urgently before this riparian ecosystem becomes disturbed beyond our ability to restore or mitigate (Allen et al., 2010; Bhatt et al., 2017). This study has resulted in the creation of high-quality bathymetric maps of both the TLD3 and TLD4 sites. The results of this study can serve as a baseline for long-term studies evaluating the pattern of water depth change over time. Prior to this study, the loss of forested upland after construction and commissioning of the TLD3 and TLD4 hydroelectric dams were not quantified. However, this study only scratches the surface of the full impact the dams have had and will continue to have on the Teesta River in the years ahead.

Valley-bottom sediment accumulation

Typically, the use of DEMs induces vertical height errors in complex topographic regions such as the site for the present study. Reasons such errors occur are due to topographic shading from camera angles (Yamazaki et al., 2017). For the MERIT DEM base map, the particulars of errors for the region were not available, and are thus not considered. Additional debris flows into the reservoirs are expected since standing water in the reservoirs has further resulted in the structural compromising of the near shore hillslope due to water ingress.

Maps of the reservoirs showing years till visible deposit formation are shown in Fig. 10. Thus, while estimates of the lifetimes may have errors, and using higher resolution and ground-corrected DEM products for re-analysis may help improve the results, we use our analysis here as indicative of significant morphological changes in the valley cross-section. Given the dynamics of sediment build-up in these reservoirs, neither of the two TLD reservoirs will be free of shallow (<3 m depth) depositional features in 90%+ of their areas well before they attain 20 years of age. This is much before the lower limit of design lifetimes (35 years) unless significant dredging-based de-silting efforts are undertaken. However, such operations are both prohibitively expensive and logistically difficult given the topography of the region. Dredging operations are also extremely detrimental to aquatic species habitats.

Preliminary (off the record) discussions with administrators of the dam operating company, NHPC Ltd., indicate that there exist no plans for dredging the full length of the reservoirs or changing the current practice of sediment flushing during high-water monsoon seasons. The latter practice just scours sediment out in the deepest part of the reservoirs in a 1–2 km stretch of the river/reservoir just upstream of the dams. Flushing operations to scour sediments during the high-flow monsoon season, from both the dams, are largely ineffective due to the tortuosity of the stream channel since both the dams are located after tight bends on the river. Current operational plans suggest flushing during monsoon rains but information from climate models has not been used to understand the effect of forecasted extreme hydrological conditions resulting from rain events either during the monsoon or during the dry season. Further, the

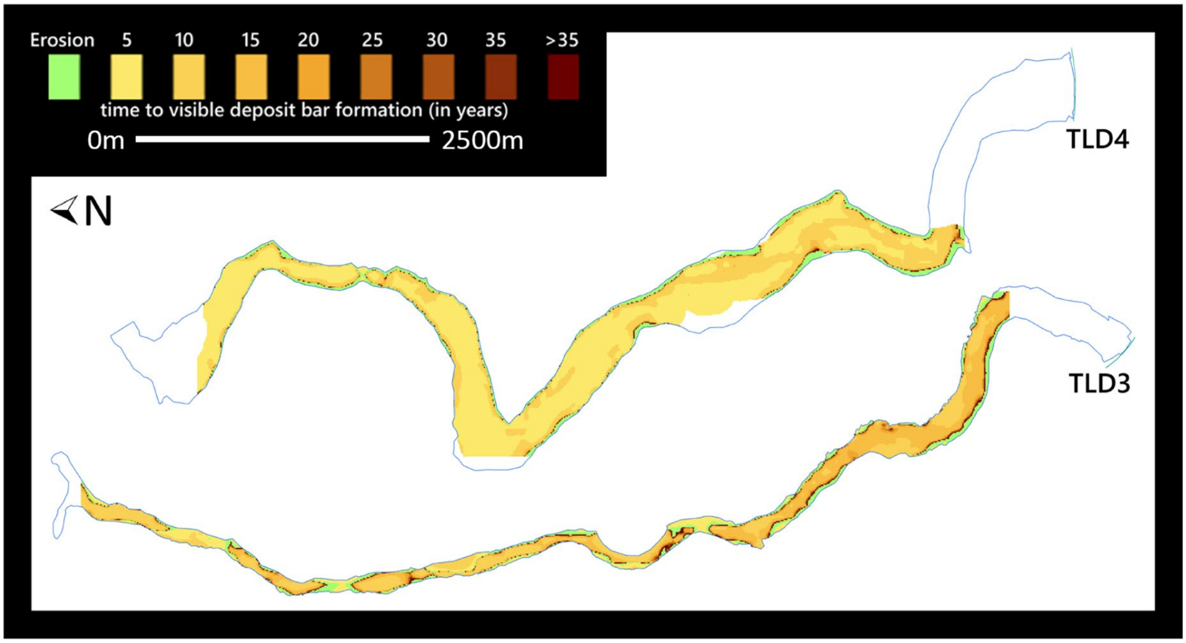

Fig. 10 Predicted number of ''years till the formation of surface visible deposition features'' (sand bars) since dam commissioning (02/2013 for TLD3, 05/2016 for TLD4)

absence of a set of continuously operated flow-meters along the river leaves the riparian and aquatic ecological conditions at peril. Additionally, there is no evidence of an assessment of the reservoir concerning its ability to deliver on biodiversity attributes other than power generation.

Thus, not only are the reservoirs at risk of becoming inefficient at water storage and thus power generation potential but there is a higher likelihood of extreme rain in the upper catchment events necessitating emergency water release due to reduced capacities. This has become even more of a threat given the increasing number of extreme rainfall events during the Indian Summer Monsoon (ISM) season in the past 4-5 decades (Goswami et al., 2006) and ensuing changing patterns of climate in the region (Ali et al. 2018).

Conclusion

The riparian vegetation community has undoubtedly been disturbed after damming. Systematic long-term monitoring and evaluation of the evolving valley morphology, dynamics of erosion-deposition processes in the catchment areas, and health of the riparian vegetation community need to be carried out. The original floodplain has been obliterated due to the formation of the dam reservoirs. The remaining riparian vegetation must be monitored carefully over time to document changes in the vegetation community and structure, including the documentation of any local extinctions of endemic species. There are significant chances of long-term changes in the species diversity and structural epithets of the riparian zone, due to the standing water in the reservoirs, and water ingress into the subsurface. A disturbed ecosystem is also vulnerable to invasion by exotic plant species given that the region is a biodiversity hotspot.

Most of the previous studies on the Teesta focus on the piedmont and downstream plains and erosion-deposition processes. A notable study by Starkel et al. (2017) did focus on the erosional processes in the exact section that we focus on, however, the study was on mechanistic fluvial morphology and the contribution of tributary streams to the morphological evolution of the river—with a baseline on the 1968 catastrophic flood event, with little quantitative evaluation of erosion-deposition amounts.

With this study of the bathymetry, we hope to offer a baseline dataset of the evolving submerged valley for future reference. The study can also be combined with sediment load metrics to offer more accurate life-cycle assessments of the reservoirs. The study also offers some idea on the changes in sediment dynamics in a valley after damming and submergence—as it pertains to the Eastern Himalaya—where a lot of dam building is ongoing.

The evolution of the soil subsurface in the vicinity of the reservoirs will be a key parameter to investigate, to understand the long-term stability of the surrounding hill-slopes and the integrity of various infrastructure in the region around the reservoirs. Such studies are also important on account of the changing dynamics of the Indian monsoon which may alter due to global climate change and additional local to regional scale micro-climatic factors. Future studies on this section of the Teesta River should include surveys of aquatic fauna. The richness, abundance, and movements of fish species post-damming of the Teesta are poorly understood. There were endangered endemic species present in the river such as the *Tor putitora* and species with little distribution and classification data such as the *Tor tor*. To date, there has been little research on these species except presence-absence studies.

From a management perspective, a continuous long-term monitoring program is needed for this river and its unique riverine and riparian ecosystem. Dam impacts can last for several decades while submerged matter decays and the local geology of the river valleys and riparian zones evolve. The impact of the dams constructed along the Teesta River cannot be fully understood through a short-term study. Further, it is critical that the dam management also include the uncertainties in the seasonality and the intensity of the ISM, which has been studied in great detail for the study area (Ali et al., 2018). Because of the nature of the dependence of hydroelectric power generators on rainfall (and hence water-head needed to turn turbines), scenarios of climate change-induced erratic patterns of rainfall need to be included in both the management of the reservoir health and in the sediment management provisions of the reservoirs. Hydrological, ecological, and pedological studies need to be conducted into the future to track changes and understand trends resulting from continual disturbance to the river dynamics of the Teesta due to dams. This study is the first of its kind to quantify the impact of dams on the Teesta River Valley in the Eastern Himalayas and serves as an important baseline data on this section of the river. Further studies monitoring the changes in both the depth, flow patterns of the Teesta River and its faunal and floral community structure are needed to fully characterize the Teesta valley's riparian ecosystem before continued disturbance causes a complete change in the riverscape.

Acknowledgements AJF was supported through Graduate Assistantship funds from the Graduate School and the Biology Department at the University of Louisiana, Monroe. JB acknowledges the generous support and funding from the Lillian L. and Fred A. Marx Endowed Professorship in Biology. NC was supported by endowments to the Suri Sehgal Centre for Biodiversity and Conservation and an endowment from the Barr Foundation. We thank Dr. Sarala Khaling, Director, ATREE Eastern Himalaya-NE India Regional Office, for hosting the researchers from UL Monroe and helping with getting field-work permits in restricted areas and in-field logistics during the field seasons in 2018-2019.

Author contributions JB conceived the idea and design of the project. AJF, NC, and JB carried out data collection, analyses, and interpretation of results. All authors contributed to the draft preparation, reviewed the results, and approved the final version of the manuscript.

Data availability The data that support the findings of this study are available from the corresponding author, [JB], upon reasonable request.

Declarations

Conflict of interest The authors declare that there is no conflict of interest that could be perceived as prejudicing the impartiality of the research reported.

References

Acharjee, M. L., & Barat, S. (2013). Ichthyofaunal diversity of Teesta river in Darjeeling Himalaya of West Bengal, India. *Asian Journal of Experimental Biological Sciences, 4*(1), 112–122.

Adhikari, D., Tiwary, R., Singh, P. P., Upadhaya, K., Singh, B., Haridasan, K. E., Bhatt, B. B., Chettri, A., & Barik, S. K. (2019). Ecological niche modeling as a cumulative environmental impact assessment tool for biodiversity assessment and conservation planning: A case study of critically endangered plant Lagerstroemia minuticarpa in the Indian Eastern Himalaya. *Journal of Environmental Management, 243*, 299–307. https://doi.org/10.1016/j.jenvman.2019.05.036

Ali, S. N., Dubey, J., Ghosh, R., Quamar, M. F., Sharma, A., Morthekai, P., Dimri, A. P., Shekhar, M., Arif, M., & Agrawal, S. (2018). High frequency abrupt shifts in the Indian summer monsoon since Younger Dryas in the Himalaya. *Scientific Reports, 8*(1), 1–8.

Allen, D. J., Molur, S., & Daniel, B. A. (2010). *The status and distribution of freshwater biodiversity in the Eastern Himalaya*. IUCN and Zoo Outreach Organization.

Aslan, A., & Middleton, V. G. (2003). Floodplain sediments. *Encyclopedia of sediments and sedimentary rocks (Encyclopedia of earth sciences series)* (pp. 285–287). Springer. https://doi.org/10.1007/978-1-4020-3609-5_88

Bhatt, J. P., Tiwari, S., & Pandit, M. K. (2017). Environmental impact assessment of river valley projects in upper Teesta basin of Eastern Himalaya with special reference to fish conservation: A review. *Impact Assessment and Project Appraisal, 35*(4), 340–350. https://doi.org/10.1080/14615517.2017.1354642

Bruun, P. (1997). Sediment transport, fluvial and marine Vol. VI, fluvial sediment transport. *Geomorphology (Encyclopedia of earth science)* (pp. 982–985). Springer. https://doi.org/10.1007/3-540-31060-6_327

Coleman, J. M. (1997). Deltaic evolution. *Geomorphology (Encyclopedia of earth science)* (pp. 255–261). Springer. https://doi.org/10.1007/3-540-31060-6_89

Fränzle, O. (1997). Valley evolution. *Geomorphology (Encyclopedia of earth science)* (pp. 1183–1189). Springer. https://doi.org/10.1007/3-540-31060-6_392

Gao, P., Wang, Z. Y., & Siegel, D. (2015). Spatial and temporal sedimentation changes in the Three Gorges Reservoir of China. *Lakes & Reservoirs, 20*(4), 233–242. https://doi.org/10.1111/lre.12109

Goswami, B. N., Venugopal, V., Sengupta, D., Madhusoodanan, M. S., & Xavier, P. K. (2006). Increasing trend of extreme rain events over India in a warming environment. *Science, 314*(5804), 1442–1445. https://doi.org/10.1126/science.1132027

Gupta, H., & Chakrapani, G. J. (2005). Temporal and spatial variations in water flow and sediment load in Narmada River Basin, India: Natural and man-made factors. *Environmental Geology, 48*(4), 579–589. https://doi.org/10.1007/s00254-005-1314-2

Harris, N., Bickle, M., Chapman, H., Fairchild, I., & Bunbury, J. (1998). The significance of Himalayan rivers for silicate weathering rates: Evidence from the Bhote Kosi tributary. *Chemical Geology, 144*(3–4), 205–220. https://doi.org/10.1016/S0009-2541(97)00132-0

The Deccan Herald (Bengaluru), India, (2015) Sikkim cut off after heavy showers. The Deccan Herald (Bengaluru), India. Retrieved 13 July, 2021, from https://www.deccanherald.com/content/486250/sikkim-cut-off-heavy-showers.html

Islam, S., & Sarker, S. C. (2017). Assessing biogeomorphological state of the Teesta River flood plain: A study on Gangachara Upazila, Rangpur, Bangladesh. *International Journal of Geosciences, 08*(02), 265–275. https://doi.org/10.4236/ijg.2017.82011

Jain, S. K., Singh, P., & Seth, S. M. (2002). Assessment of sedimentation in Bhakra reservoir in the western Himalayan region using remotely sensed data. *Hydrological Sciences Journal, 47*(2), 203–212. https://doi.org/10.1080/02626660209492924

Kiss, T., Fiala, K., & Sipos, G. (2008). Alterations of channel parameters in response to river regulation works since 1840 on the Lower Tisza River (Hungary). *Geomorphology, 98*(1–2), 96–110. https://doi.org/10.1016/j.geomorph.2007.02.027

Malini, B. H., & Rao, K. N. (2004). Coastal erosion and habitat loss along the Godavari delta front—a fallout of dam construction (?). *Current Science, 87*(9), 1232–1236.

Marsh, G. A., & Fairbridge, R. W. (1999). Lentic and lotic ecosystems. *Environmental geology* (pp. 381–388). Springer. https://doi.org/10.1007/1-4020-4494-1_204

Mehta, S. (2013). Map of proposed dams in the Teesta River Basin. Retrieved 13 July, 2021, from https://sandrp.files.wordpress.com/2018/03/teesta-150411.jpg

Myers, N., Mittermeier, R. A., Mittermeier, C. G., Da Fonseca, G. A., & Kent, J. (2000). Biodiversity hotspots for conservation priorities. *Nature, 403*(6772), 853–858. https://doi.org/10.1038/35002501

Nanson, G. C., & Gibling, M. R. (2013). Rivers and alluvial fans. *Encyclopedia of sediments and sedimentary rocks (Encyclopedia of earth sciences series)* (pp. 568–583). Springer. https://doi.org/10.1007/978-1-4020-3609-5_173

Olofin, E. A. (1988). Short communications monitoring the impact of dams on the downstream physical environment in the tropics. *Regulated Rivers, 2*(2), 167–174. https://doi.org/10.1002/rrr.3450020210

Pal, R., Biswas, S. S., Pramanik, M. K., & Mondal, B. (2016). Bank vulnerability and avulsion modeling of the Bhagirathi-Hugli river between Ajay and Jalangi confluences in lower Ganga Plain, India. *Modeling Earth Systems and Environment, 2*(2), 65. https://doi.org/10.1007/s40808-016-0125-7

Panda, D. K., Kumar, A., & Mohanty, S. (2011). Recent trends in sediment load of the tropical (Peninsular) river basins of India. *Global and Planetary Change, 75*(3–4), 108–118.

Petley, D. N. (2013). Characterizing giant landslides. *Science, 339*(6126), 1395–1396. https://doi.org/10.1126/science.1236165

Pradhan, S. P., Vishal, V., & Singh, T. N. (2015). Study of slopes along River Teesta in Darjeeling Himalayan region. *Engineering geology for society and territory* (Vol. 1, pp. 517–520). Springer. https://doi.org/10.1007/978-3-319-09300-0_97

SANDRP. (2020). Landslide in Sikkim damages NHPC's Teesta V dam project. Retrieved 13 July, 2021, from https://sandrp.in/2020/06/27/landslide-on-nhpcs-teesta-v-project-in-sikkim-damages-the-dam/

Schmudde, T. H. (1997). Flood plain. *Geomorphology (Encyclopedia of earth science)* (pp. 359–362). Springer. https://doi.org/10.1007/3-540-31060-6_131

Seret, G. (1997). Fluvioglacial processes. *Geomorphology (Encyclopedia of earth science)* (pp. 362–366). Springer. https://doi.org/10.1007/3-540-31060-6_132

Sinha, A. (2020). Four landslides block NH10. The telegraph (Kolkata), India. Retrieved 13 July, 2021, from https://www.telegraphindia.com/west-bengal/four-landslides-block-nh10/cid/1792871

Starkel, L., Wiejaczka, Ł, & Kiszka, K. (2017). Role of tributaries in shaping the middle course of the Himalayan River Teesta after the 1968 extreme floods. *Current Science, 112*(9), 1896. https://doi.org/10.18520/cs/v112/i09/1896-1903

Wiejaczka, Ł, Piróg, D., Tamang, L., & Prokop, P. (2018). Local residents' perceptions of a dam and reservoir project in the Teesta Basin, Darjeeling Himalayas, India. *Mountain Research and Development, 38*(3), 203–210. https://doi.org/10.1659/MRD-JOURNAL-D-16-00124.1

Willis, C. M., & Griggs, G. B. (2003). Reductions in fluvial sediment discharge by coastal dams in California and implications for beach sustainability. *The Journal of Geology, 111*(2), 167–182. https://doi.org/10.1086/345922

Yamazaki, D., Ikeshima, D., Tawatari, R., Yamaguchi, T., O'Loughlin, F., Neal, J. C., Sampson, C. C., Kanae, S., & Bates, P. D. (2017). A high-accuracy map of global terrain elevations. *Geophysical Research Letters, 44*(11), 5844–5853. https://doi.org/10.1002/2017GL072874